



This is the accepted version of this paper. The version of record is available at <https://doi.org/10.1016/j.envpol.2022.120200>

1 **Relevance of tyre wear particles to the total content of microplastics transported by**
2 **runoff in a high-imperviousness and intense vehicle traffic urban area.**

3
4
5
6 Luiza Ostini Goehler¹, Rodrigo Braga Moruzzi^{1*}, Fabiano Tomazini da Conceição¹, Antônio
7 Aparecido Couto Júnior², Lais Galileu Speranza^{1,3}, Rosa Busquets^{4,5}, Luiza Cintra Campos⁵

8
9
10
11 1 - UNESP - Universidade Estadual Paulista, Instituto de Ciência e Tecnologia de São José dos
12 Campos - ICT, São José dos Campos, Brazil.

13 2 – RAM Consultoria e Assessoria Ambiental Ltda, Rio Claro, Brazil.

14 3 – GreenCoLab – Associação Oceano Verde, Faro, Portugal.

15 4 – School of Life Sciences, Pharmacy and Chemistry, Kingston University, United Kingdom.

16 5 - Department of Civil, Environmental and Geomatic Engineering, University College
17 London, United Kingdom.

18
19
20
21 **Corresponding author:**

22 * UNESP, IGCE, Avenida 24-A, 1515, CEP: 13506-900, Rio Claro, São Paulo, Brasil. Tel: +55
23 19 5326-9339. E-mail: rodrigo.moruzzi@unesp.br

Abstract

25
26
27
28
29
30
31
32
33
34
35
36
37
38
39
40
41
42
43
44
45
46
47
48
49
50
51

Microplastics (MPs) are an emerging pollutant and a worldwide issue. A wide variety of MPs and tyre wear particles (TWPs) are entering and spreading in the environment. TWPs can reach waterbodies through runoff, where main contributing particulate matter comes from impervious areas. In this paper, TWPs and other types of MPs that were transported with the runoff of a high populated-impervious urban area were characterised. Briefly, MPs were sampled from sediments in a stormwater detention reservoir (SDR) used for flood control of a catchment area of ~ 36 km², of which 73% was impervious. The sampled SDR is located in São Paulo, the most populated city in South America. TWPs were the most common type of MPs in this SDR, accounting for 53 % of the total MPs; followed by fragments (30 %), fibres (9 %), films (4 %) and pellets (4 %). In particular, MPs in the size range 0.1 mm-0.5 mm were mostly TWPs. Such a profile of MPs in the SDR is unlike what is reported in environmental compartments elsewhere. TWPs were found at levels of 2,160 units/(kg sediment·km² of impervious area) and 87.8 units/(kg sediment·km street length); MP and TWP loadings are introduced here for the first time. The annual flux of MPs and TWPs were 7.8x10¹¹ and 4.1x10¹¹ units/(km²·year), respectively, and TWP emissions varied from 43.3 to 205.5 kg/day. SDRs can be sites to intercept MP pollution in urban areas. This study suggests that future research on MP monitoring in urban areas and design should consider both imperviousness and street length as important factors to normalize TWP contribution to urban pollution.

Keywords: Microplastic pollution; High urbanization; Imperviousness; Environmental management.

52 1. Introduction

53

54 Microplastics (MPs) are defined as plastic particles ranging from 1 μm to 5 mm (Frias
55 and Nash, 2019). They commonly originate from products such as textile, plastic waste,
56 pigment particles or some personal care products (Skaf et al., 2020). The MPs have different
57 sizes, shapes, colours, compositions and density, and the well-established high stability of
58 polymer constituents of MPs, increases and prolongs their negative impact in the environment
59 (Anbumani and Kakkar, 2018; Ma et al., 2020). Furthermore, MPs may transport toxic organic
60 chemicals, heavy metals and microorganisms that could affect aquatic organisms, and some
61 have the potential for bioaccumulation and biomagnification (Ma et al., 2019; Kumar et al.,
62 2021).

63 MPs tend to be at high levels in areas with large population worldwide (Bronwe et al.,
64 2011; Vaughan et al., 2017; Jiang et al., 2019, Nematollahi et al., 2022), due to the generation
65 of high amounts of litter with non-appropriate waste disposal and high number of vehicles (Li
66 et al., 2020; Koutnik et al., 2021). The escalation in population density, associated with
67 urbanisation, is associated with an increase in impervious areas (Ramezani et al., 2021;
68 Kawakubo et al., 2019; Wu et al., 2020), which subsequently affects the response of an area
69 after a rainfall events, typically increasing runoff in the area (Miller et al., 2014; Huang et al.,
70 2008; Jacobson, 2011). Runoff from storms washes out impervious surfaces in densely
71 populated areas, carrying the previous build-up of plastics and its degradation products into
72 water bodies (Triebkorn et al., 2019; Grbić et al., 2020; Lange et al., 2021; Smyth et al., 2021).

73 Brazil is considered one of the most urbanised medium-income countries in the world
74 (Lima and Rueda, 2018). São Paulo, with 12,396,372 inhabitants (Brasil, 2022), is the largest
75 city in Brazil, second largest city in Latin America and the sixth most populous city in the
76 world. São Paulo has an urbanisation rate of 99.1 % (Collaço et al., 2019). When urbanisation

77 arises from a poorly controlled occupation process, as in São Paulo, impervious surfaces reach
78 high levels (above 50 %) (Martins et al., 2018), resulting in high volume runoffs and frequent
79 floods (Lima et al., 2018; Simas and Rodrigues, 2020). Flood events are intensified by climate
80 conditions, and these promote transport of MPs.

81 Stormwater detention reservoirs (SDRs) have been used as an engineered solution to
82 minimise impacts of flooding (Santos and Mazivieiro, 2016), by equalising the runoff volume
83 during rainfall events (Szelag et al., 2019), especially in South-Eastern Brazilian states. After a
84 rainfall event, the accumulated rainwater is pumped out of SDRs back to the river, and this
85 leaves different solid materials remaining at the bottom of the reservoir. SDRs differ across
86 previous studies (Lin et al., 2021; Niu et al., 2022; Koutnik et al., 2022) because these SDRs
87 relate to different impervious surface and operational conditions. SDRs were indicated by the
88 team as potential hotspots for MPs, which are found in large number and variability in such
89 sites (Moruzzi et al., 2020).

90 While fibres are reported by different monitoring studies to be the dominant MPs in
91 urban areas (Nematollahi et al 2022), tyre wear particles (TWPs) have the potential to become
92 one of the largest type of MPs¹. In addition, TWPs have been found in the environment and can
93 be a risk to ecosystems and human health (Wik and Dave, 2009; Halle et al., 2021). This paper
94 primarily assesses the relevance of TWPs to the total content of MPs in an urban area with high
95 imperviousness and vehicle traffic. This is an urban characteristic that can be relevant to the
96 understanding of different pathways taken by MP pollution to the environment that has not yet
97 been addressed in previous studies. For this purpose, samples of sediments transported by urban
98 runoff were collected from the bottom of the Jardim Arize SDR, municipally of São Paulo, and
99 MPs, including TWPs, were characterised.

¹ Here we adopt the general definition of MP proposed by Verschoor (2015), which accounts MP as all man-made macromolecular material, including synthetic rubber.

100 2. Material and Methods

101

102 2.1. Study area description

103 The city of São Paulo created the Flood Control Programme in the Aricanduva River
104 basin in the 1990s as a way of reducing and/or minimizing the impacts of floods over vulnerable
105 population during intense rainfall events in the region. This involved implementation of flood
106 storage reservoirs on or adjacent (in-line or off-line types) to the Aricanduva River and its
107 tributaries. The Aricanduva River basin has high impervious surface rates and a long history of
108 flooding (Simas and Rodrigues, 2020). In addition, the traffic in the area reaches one the highest
109 loading of vehicles in São Paulo city with values as high as 24,700 vehicles/day in the main
110 arterial road only (CET, 2019).

111 The Jardim Arize SDR (23°33'42.10" S and 46°30'35.92" W), built in 2002 (Canholi,
112 2014), is located in the Aricanduva River basin. This SDR drains an area of 36.437 km² (Fig.
113 1), with 390,614 inhabitants and an average of demographic density and Human Development
114 Index (HDI) of 10,723 inhabitants/km² and 0.79, respectively (São Paulo, 2017). The Jardim
115 Arize SDR is an engineered structure, which operates as an off-line SDR with total capacity of
116 160,000 m³ (17,750 m² and average depth of 9 m). It was designed to reduce the Aricanduva
117 River flow from 94 m³/s to 75 m³/s, for a rainfall of 10 years of return period (TR) (Canholi,
118 2014). Stormwater comes from a side weir, positioned in the middle length of the SDR. The
119 weir is set at a level that watercourse can accommodate flow at normal period. During a rainy
120 period, any additional flow, established from the maximum level for critical stormwaters,
121 passes over the weir into the SDR. The flow then spread quickly over the SDR area, and stays
122 until the end of the critical rainfall period, where detained water is pumped out back to the
123 watercourse. The sediment brought by the flow remains at the SDR bottom and is scratched and
124 put aside for removal. Lorries can then remove the sediment to a controlled landfill as final

125 destination. The cycle is then repeated for new critical stormwaters and the frequency of
 126 cleaning depends upon the amount of sediment carried by the runoff. Figure 2 shows the
 127 schematic sequential operation for the Jardim Arize SDR. The climate of the study area is
 128 classified as humid tropical, with wet summer (October to March) and dry winter (April to
 129 September) (Simas et al., 2017).

130

131 2.2. Land use description, hydrological settings and SDR sediments

132 The land-use mapping of the catchment area was performed as outlined by Lupinacci et
 133 al. (2017, 2022) and Couto Júnior et al. (2019), consisting of a visual interpretation of satellite
 134 images acquired from Sentinel 2A. The following land-use classes were mapped: (i) water
 135 bodies, (ii) permeable areas (reforested areas, exposed soil and unoccupied areas), and (iii)
 136 impervious areas (residential/commercial and industrial areas), which are areas of intensive use
 137 and include buildings and road systems. The total street length was also calculated from the
 138 land use mapping.

139 The region of São Paulo city has the average annual rainfall between 1300 mm and 1500
 140 mm (Lima et al, 2018). The average monthly and annual rainfall in the study area was quantified
 141 using data from the E3-035 rainfall station (23°39'04" S and 46°37'2" W) from 1936 to 2019
 142 (DAEE, 2020). The rainfall intensity for different TR (in years) was obtained using Equation 1
 143 (DAEE, 2018), for $10 \leq d \leq 1440$ min.

144

$$145 \quad I = 32.77(d + 20)^{-0.8780} + 16.10(d + 30)^{-0.9306} \left[(-0.4692 - 0.8474 \ln(\ln(\frac{TR}{TR-1})) \right] \quad (1)$$

146 where I is rainfall intensity (mm/min) and d is rainfall duration (min).

147

148 Rainfall intensities, responsible for the runoff and washing out of MPs and TWPs, for
 149 the sampling period were assessed. For this, data from two rainfall stations, namely Interlagos

150 (23°43'28" S and 46°40'39" W) and Henry Borden (23°42'11" S and 46°40'26" W) were
151 evaluated from January to August 2019, according to the dataset available at Water and Energy
152 Department's database (DAEE, 2020). Finally, data related to the composition of residues,
153 collected monthly from the studied SDR, in tonnes (AMLURB, 2022), were used to quantify
154 the amount of accumulated sediment.

155

156 *2.3. Sampling and microplastics separation*

157 Sediment samples were collected from Jardim Arize SDR (23°33'42.10" S and
158 46°30'35.92" W) (Fig. 3a). The reservoir operates intermittently, according to the runoff flow,
159 and samples were taken when the Jardim Arize SDR was without water (in August 2019). Two
160 superficial sediment samples (2 kg) were collected at the bottom of SDR (Fig. 3b), equidistant
161 50 m from the weir, corresponding to the 2nd and 3rd quartile for length, at the central position
162 of SDR's width, covering the entire depth (~ 50 cm). A preliminary analysis did not find
163 difference ($p < 0.05$) in the profile of MPs across sampling positions. Also, due to the operational
164 characteristics in the Jardim Arize SDR, every sediment sample collected results from the
165 transport of sediment from various rainfall events. Hence, the content of the SDR is itself a
166 composite sample (Fig. 2). The samples were then stored in sealed glass containers and
167 transported to the laboratory.

168 The sediment samples were dried at room temperature and from each sample, three
169 representative fractions (30 g each) were collected, totalising six samples where MPs and TWPs
170 were quantified. Each sample was added to a glass beaker with 300 mL of a solution containing
171 water and $ZnCl_2$ (> 98 %, from Sigma-Aldrich, Brazil) dissolved at a density of 1.6 g/cm³. The
172 mixture was manually homogenized, transferred to the Imhoff cone and after 24 h of
173 sedimentation, the supernatant water was filtered through a 0.45 μm cellulose nitrate
174 membranes filter with 47 mm of diameter (Sartorius, Brazil). A blank sample consisting of the

175 same amount of free-plastic soil was treated in parallel to monitor potential contamination by
176 new microplastics from the laboratory environment during the procedure.

177

178 *2.4. Quantification and characterization of microplastics*

179 After use, the membrane filters were placed in closed glass petri dishes for drying
180 (around 23 °C for at least 24 h) and subsequent quantification and characterization of all MPs
181 and TWPs, followed the procedures outlined by Moruzzi et al. (2020). The TWPs, among the
182 MPs found in the sediment samples, were identified using visual criteria, as performed by Leads
183 and Weinstein (2019). TWPs are black particles, elongated/cylindrical in shape, may be
184 partially covered with other road impurities, and have a rough surface and rubber consistency,
185 which remains even when handled with tweezers. MPs and TWPs were visually identified and
186 counted using a stereo microscope (Zeiss Discovery V12 SteREO, Germany) with an integrated
187 camera (AxioCam ER 5s, Germany). The particles were classified into categories according to
188 their type (fibres, films, fragments, pellets and tyres) and size (0.1 mm to 0.5 mm, 0.5 mm to
189 1.0 mm and 1.0 mm to 5.0 mm). Particles lower than 0.1 mm were not considered because of
190 limitations of the light microscope used. MPs in the samples were counted as the number of
191 MPs per kilogram of sediment (units/kg). Preliminary tests were set to confirm the main TWP
192 characteristics, and colour was found to be a remarkable trait for visual inspection. Random
193 samples of black particles were then taken and TWPs were confirmed by ATR FT-IR (Varian
194 640-IR, Netherlands) with spectra from 400 – 4000 cm^{-1} , comparing the spectra obtained with
195 an online database (Bio-Rad Sadtler, Brazil). Additionally, the morphology and composition
196 (presence of sulfur) of TWPs was characterized using Scanning Electrical Microscopy with
197 Energy Dispersive X-Ray Spectroscopy (SEM-EDS) (JEOL - JSM-6010 LA, USA), which
198 confirmed the presence of sulfur in the specimens.

199

200

201 *2.5. Annual flux and emission factor*

202 The annual flux of MPs (F_{MPs}) and TWPs (F_{TWPs}) were determined using Equation 2,
 203 considering the total loading of sediments to SDRs for the catchment area.

204

$$205 \quad F_{MPs} \text{ or } F_{TWPs} = \frac{C \cdot S}{A} \cdot 10^3 \quad (2)$$

206 where F_{MPs} and F_{TWPs} stand for annual flux of MPs and TWPs [units/(km².year)], respectively;

207 S is the total mass of sediments (t/year); C is either the MPs or TWPs (units/kg); A is the

208 catchment area (km²), being the ratio C/A the loading of MPs or TWPs [units/(kg.km²)].

209

210 The TWP emission factor within the catchment area (T_{TWP} in kg/day) was estimated

211 through the Equation 3 (Järllskog et al., 2020). The F_{tw} for the type of vehicle was based on Kole

212 et al. (2017) and NV obtained from CET (2019), based on 13 peak hours for the study area. The

213 peak hours represent the time interval between 7 am and 8 pm, where most of the vehicle traffic

214 concentrates. For the L_C , only the arterial roads, which receive the highest volume of vehicle

215 traffic, were considered.

216

$$217 \quad T_{TWP} = F_{tw} \cdot NV \cdot L_C \cdot 10^3 \quad (3)$$

218 where F_{tw} is the emission factor of tyre wear particles [kg/(vehicle.km)]; NV is the annual

219 average of daily traffic (vehicles/day); and L_C is the street length of arterial roads within the

220 catchment area (km).

221

222

223

224

225 **3. Results**

226

227 *3.1. Land use mapping*

228 The land-use mapping of the catchment area is presented in Figure 4. The
229 residential/commercial areas (52.67 %) are the main land-use in the study area, followed by
230 industrial areas (20.37 %) and reforest (15.32 %) (Table S1). The impervious area was 26.60
231 km² in 2019, which represented ~ 73 % of the total study area. In 2019, the total street length
232 of the study area was 640 km, with a street density of 24 km/km². The arterial roads sum 65.9
233 km and cross the catchment area from East to West mostly.

234

235 *3.2. Rainfall characteristic of the catchment area*

236 The annual rainfall average was 1,437.1 mm, with the annual rainfall values ranging
237 from 887 mm (1963) to 2,228 (1983) in the study area over 80 years (Fig. S.1a). The monthly
238 average rainfall was 119.9 ± 68.9 mm, with January (237.6 ± 91.1 mm) being the rainiest month
239 and August (37.8 ± 33.0 mm) the driest (Fig. S.1b). Figure S.1c, derived from Equation 1,
240 indicates rainfall intensities expected for different durations and TRs. For TR between 2 and 10
241 years, rainfall intensities up to 63 mm/h are expected, with duration of 60 min, while ~ 94 mm/h
242 are estimated for TR of 10 years and duration of 30 min. Lower intensity rainfalls, with
243 intensities < 54 mm/h, are more likely to occur with TR values (TR < 5 years). The maximum
244 registered rainfall intensity during the sampling period was 56 mm/h, corresponding to TR of
245 6 years (Table S.2), with 84 % chance to be equalled or surpassed within 10 years.

246

247 *3.3. SDR's sediments*

248 The monthly average mass of sediments removed from the SDRs in São Paulo is shown
249 in Figure S.2, where the data was compiled from AMLURB (AMLURB, 2022). The quantity

250 of sediments removed from the SDR was $15,900 \pm 976$ tonnes/month on average, ranging from
251 $14,280 \pm 1,680$ tonnes (in January, average 2013-2020) to $18,421 \pm 6,150$ tonnes (in December,
252 average 2013-2020). The sediments are collected by the municipal cleaning service and
253 deposited in controlled landfills engineered with necessary civil structures to prevent soil and
254 groundwater contamination.

255

256 *3.4. MP quantification and characterisation*

257 The total amount of MPs (unit/kg), including TWPs, found in the Jardim Arize SDR is
258 presented in Table 1. Figure 5 shows the distribution of MPs by type and size. MPs in the
259 sediment samples from the Jardim Arize SDR were 109,089 units/kg, with TWPs being the
260 most common MPs (57,461 units/kg), followed by fragments (32,456 units/kg), fibres (10,022
261 units/kg), films (4,622 units/kg) and pellets (4,528 units/kg) in that order. Figure 6 shows
262 representative examples of different MPs. Optical microscopy images (Fig. 7a and 7b) and SEM
263 micrographs (Fig. 7c) illustrate typical rough surfaces of TWPs. In addition, the
264 characterization with FTIR confirmed that the particles identified were tyre fragments (Fig. 7d).
265 The MPs detected on the Jardim Arize SDR were mainly 0.1 to 0.5 mm (~ 90 %), followed by
266 MPs ranging from 0.5 mm to 1.0 mm (~ 6 %) and 1.0 mm to 5.0 mm (~ 4 %), being 0.1 mm
267 the lowest size that the methodology used in this work allowed to study. TWPs prevailed with
268 57 % of the MPs size ranging from 0.1 mm to 0.5 mm.

269

270 *3.5. Annual flux and emission factor*

271 Based on the average of 190,800 t of sediment/year deposited on the SDRs (Fig. S.2),
272 compiled from the database presented by AMLURB (2022), the annual flux of MPs and TWPs
273 were 7.8×10^{11} and 4.1×10^{11} units/(km².year), respectively. For the T_{TWP} , Brazilian F_{tw} values
274 for mass of tyre debris per vehicle and kilometre were used for calculation, according to Kole

275 et al. (2017): 0.132 g/(vehicle.km) for automobiles, 0.007 g/(vehicle.km) for motorcycles, 1.068
276 g/(vehicle.km) for trucks and 0.204 g/(vehicle.km) for buses. The NV was considered in the
277 range of 5,200 – 24,700 vehicles/day (CET, 2019). The percentage of each vehicle category
278 was 79.10 % for cars, 15.74 % for motorcycles, 1.37 % for trucks and 2.99 % for buses. The L_C
279 was 65.91 km within 640 km. Finally, the T_{TWP} was estimated from 43.3 to 205.5 kg/day
280 depending on the daily vehicle traffic.

281

282 **4. Discussion**

283

284 *4.1 Rainfall characterisation and SDR sediments for the sampling period*

285 Figure S.2 indicates that the average amount of sediments removed monthly from the
286 SDRs in São Paulo city from 2013 to 2020 had low variation with time. As such, sediments that
287 accumulated at the bottom of São Paulo SDRs were approximately removed at a constant rate,
288 regardless of the season, following operational and logistic arrangements. While this can be
289 considered a disadvantage for a paired relation analysis between rainfall and sediment transport,
290 it provides a more homogeneous sample for the assessment of the long-term accumulation of
291 MPs and allows for a more consistent evaluation of representative samples.

292

293 *4.2 Comparison of total amount of microplastics in different sites in Brazil and elsewhere*

294 A summary of the total amount of MPs identified in sediments from sites close to urban
295 areas (in Brazil and elsewhere) is presented in Table 2. Previous studies indicate great variation
296 in the number of MPs, depending on the sampling point. For instance, MPs measured by Zheng
297 et al. (2020) in China was ≤ 20 units/kg, whilst values ranging from ≤ 80 to $\leq 3,763$ units/kg
298 were found in streams and river from New Zealand (Dikareva and Simon, 2019) and Germany
299 (Klein et al., 2015). On the other hand, ponds and lakes may present values as high as $\sim 28,000$

300 (Liu et al., 2019) or 128,000 units/kg (Ballent et al., 2016). The reason for such variation comes
301 not only from social and environmental aspects (Ballent et al., 2016; Zhang et al., 2020), but
302 also specific characteristics of the water bodies and reservoirs sampled. The volume of water
303 bodies and reservoir characteristics are expected to bring down the total amount of MPs brought
304 by runoff. Rivers, lakes and ponds may have multiple inlet contribution (tributaries) as well as
305 having multipurpose uses (e.g. drinking water source, energy generation, etc).

306 A previous study showed MPs in a Brazilian SDR of ~ 57,500 units/kg (Moruzzi et al.,
307 2020), whereas the present work has found ~ 109,000 units/kg, possibly because the catchment
308 area and land use differ from one another. Although the levels of MPs found were very different
309 than this study, the high total content of MPs on the SDR confirms that stormwater reservoirs
310 are hotspots of MPs and should be more investigated and used to intercept MP pollution. The
311 presence of MPs in multipurpose reservoirs not designed specifically for flood control but for
312 other uses - such as water supply, irrigation and power generation - has also been reported (Niu
313 et al., 2022; Di and Wang, 2018; Lin et al., 2021). Furthermore, unlike most of SDRs deployed
314 in the municipally of São Paulo, these reservoirs are not impervious tanks, so the particles can
315 infiltrate into soil. Therefore, SDRs are adequate for the assessment of the abundance and
316 characterization of MPs transported by runoff in impervious catchment areas, as they are
317 designed to contain flood and built with an impermeable bottom (Santos and Mazivieiro, 2016),
318 thus acting as a barrier for these particles (Moruzzi et al., 2020).

319

320 *4.3. Different sizes and types of MPs*

321 Except for pellets, which were exclusively found in the size ranging between 0.1 and
322 0.5 mm (where 0.1 mm was the smallest MPs analysed), the distribution of MPs in this lowest
323 size range constitutes 90 % of the total MPs. This is in accordance with previous investigations
324 in sediment samples reported by Moruzzi et al. (2020), Lin et al. (2021), Zheng et al. (2020)

325 and Nematollahi et al. (2022). In addition, TWPs prevailed in the size ranging from 0.1 to 0.5
326 mm, as they are more easily transported from pathways by high-frequency surface runoff, while
327 larger particles (> 0.5 mm) require higher flows and can also be trapped in the environment
328 close to the pathways where they are generated (Järnskog et al., 2021; Klöckner et al., 2020).

329 It is noticeable that a great number of MPs come from TWPs. TWPs were the main
330 contributors to MPs in the studied SDR. Relevance of TWPs in the total content of MPs has
331 been described by few studies in Australia (Ziajahromi et al., 2020), Sweden (Järnskog et al.,
332 2021) and USA (Leads and Weinstein, 2019; Werbowski et al., 2021). TWPs are generated by
333 the friction between the tyre and the road surface (Knight et al., 2020) and are made from natural
334 and synthetic rubber (polyisoprene or styrene-butadiene rubber) (Järnskog et al., 2020). The
335 magnitude of TWP release is related to the number of vehicles (Wik e Dave, 2009) and depends
336 upon the tyre and road characteristics (composition and conservation conditions),
337 imperviousness of the catchment area and environmental factors, such as weather conditions
338 and driving style (Zhang et al., 2020; Yan et al., 2021). Street length can play an important role
339 on emission levels of TWPs alongside the traffic load, which is why normalized pollution levels
340 are herein proposed. Finally, atmospheric movement and deposition may also affect the
341 distribution of MPs and TWPs (Koutnik et al., 2022) (Sun et al., 2022; Li et al., 2022; Koutnik
342 et al., 2021). However, it is likely that wet regions are more prone to be influenced by TWPs
343 from emissions from traffic, where runoff may modulate MP transport during rainy period, as
344 shown by de Carvalho et al. (2022).

345 Fragments were the second most abundant MP type (30 %) found in the Jardim Arize
346 SDR. Large amounts of MP fragments (from 50 to 70 %) have also been reported by several
347 authors (Moruzzi et al., 2020; Ballent et al., 2016; Dirakeva and Simon, 2019; Niu et al., 2022).
348 Given that TWPs can also be classed as fragment, some discrepancies in the proportions of the
349 type of MPs were expected. Since fragments originate from the degradation of solid waste and

350 other larger plastics (Horton et al., 2017; Akdougan and Guven, 2019), their presence in greater
351 amounts in densely populated places, where there is also greater use of plastic products, is
352 expected (Browne et al., 2011; Jiang et al., 2019).

353 Fibres accounted for 9 % of the total MPs observed in this study, which is consistent
354 with the value reported by Moruzzi et al. (2020) in another Brazilian SDR, in the municipally
355 of Poa. Their abundance increased with size (0.5 mm to 1.0 mm, 35 %), becoming predominant
356 in the range of 1.0 mm to 5.0 mm (55 %). Fibres have been the dominant MPs in other urban
357 areas, such as in Three Gorges Reservoir sediments, China (Di and Wang, 2018), in Lake
358 Bolsena and Chiusi sediments, Italy (Fischer et al., 2016), in Jiaozhou Bay sediments, China
359 (Zheng et al., 2020), in Danjiangkou Reservoir sediments, China (Lin et al., 2021), in Ahvaz
360 soil samples, Iran (Nematollahi et al., 2022) and in Tibet Plateau sediment, China (Jiang et al.
361 (2019). The sources of fibres are mainly textile products, such as clothing and carpets (Bronwe
362 et al., 2011), mainly due to the discharge of effluents from washing machines (Dris et al., 2018).
363 Therefore, higher percentages of fibres are expected in combined systems or separated sewage
364 systems. However, since the beginning of the 20th century, Brazil has had separated systems,
365 i.e. stormwater and sewage are collected by different pipes. This may show that SDRs in urban
366 areas are capturing different pollution aspects from other types of reservoirs, soils, lakes, rivers
367 and bays.

368 Films, accounting for 4 % of total MPs (Fig. 5a), were more prominent in the larger
369 defined size ranges of MPs (representing 18 % in the range of 0.5 mm – 1.0 mm and 17 %
370 within 1.0 – 5.0 mm). Films are secondary MPs from plastic waste, with a characteristic thin
371 layer morphology, generated from the fragmentation of packaging materials and plastic
372 containers (Di and Wang, 2018), and are also expected in greater abundance in places with high
373 population density and use of plastic products.

374 Finally, pellets were among the lowest concentrations on MPs measured in this work (4
375 %) and is in agreement with the literature (Rodrigues et al., 2018; Lin et al., 2021; Di and Wang,
376 2018; Jiang et al., 2019; Moruzzi et al., 2020). However, is not in keeping with the well-
377 established greater importance that pellets/beads acquired in the mass media communication,
378 and their subsequent restructured use in personal care products in some countries. Indeed,
379 pellets primarily come from cosmetics industry and hygiene products (Di and Wang, 2018;
380 Jiang et al., 2019).

381

382 *4.4. Influence of imperviousness, street length and vehicle traffic on the content of MPs and* 383 *TWPs*

384 MP pollution, like other type of pollution, tends to be high in urban areas (Vaughan et
385 al., 2017), and there is a clear variation in the characteristics of such pollution between rural
386 and urban areas (Di and Wang, 2018). In addition to the input and movement of contaminants
387 (Grbić et al., 2020), the structure of the urban areas and vehicle traffic influence the quantity
388 and transport of MPs in the area (Järlskog et al., 2021). Urbanization is also related to the
389 increase of impervious surfaces (Rameziani et al., 2021; Wu et al., 2020) and total street length
390 (Peponis et al., 2007), both being factors with high potential to influence the transport of MPs,
391 including the total content of TWPs.

392 The Aricanduva watershed has a high-impervious surface, high demographic density,
393 and also 640 km of street length. These characteristics are similar to other parts of São Paulo
394 for low-income occupation (Sobrinho and Tsutiya, 1999), but may be very different from
395 wealthier areas that have better infrastructure and lower demographic density. Both,
396 imperviousness and street length are related to tyre wear. They both may help to understand
397 TWP pathway from similar urban conditions in Brazil or elsewhere. In this study, the total
398 amounts of MPs and TWPs were normalized by the total impervious area (km²) and the total

399 street length (km), resulting in 4,101 units/(kg·km²) and 170.5 units/(kg·km) for MPs, and 2,160
400 units/(kg·km²) and 87.8 units/(kg·km) for TWPs. Such normalized data has not been presented
401 in previous studies and this work constitutes the first recommendation for MPs in urban
402 environments.

403 In addition, the abundance of MPs and TWPs in the Jardim Arize SDR ranging from 0.1
404 mm to 0.5 mm may be explained by the high residential imperviousness area and frequency of
405 moderate to low rainfall intensities (low TR), with small particles being easily transported by
406 low overland flows. Previous studies have also shown the importance of runoff for the transport
407 and occurrence of MPs in areas with high impervious surface (Hong et al., 2016; Strobach et
408 al., 2019; Triebkorn et al., 2019; Grbić et al., 2020; Wu et al., 2020; Lange et al., 2021;
409 Rameziani et al., 2021; Smyth et al., 2021). High-impervious areas such as Jardim Arize
410 increase the effect of runoff on MPs and TWPs transport, and also facilitates the interpretation
411 of the MPs pollution at SDRs.

412 The annual flux of MPs and TWPs were 7.8×10^{11} and 4.1×10^{11} units/(km²·year),
413 respectively, for 190,800 t of sediment/year deposited in SDRs (AMLURB, 2022). Although
414 from different sources, the annual flux obtained has the same order of magnitude as those
415 presented by Dris et al. (2018). The lack of data on this topic is still a challenge and the
416 heterogeneity of sources and types of MPs makes comparisons difficult. However, the results
417 presented here may assist future researchers in assessing MP pollution. Finally, the T_{TWP} values
418 estimated in this study (43.3 to 205.5 kg/day), based on local data, are much higher than the
419 0.81 kg/year reported by Kole et al. (2017), who considered the TWP generation data, global
420 vehicles and population. Apparently, in densely populated areas, such as the city of São Paulo,
421 there is a significant increase of the TWP emission due to imperviousness and street length,
422 associated with the vehicle traffic. Future research should address the effect of the type of road
423 on the emission of TWP.

424 **5. Conclusions**

425

426 The study area located in the municipality of São Paulo covered 36 km², 73 % of which
427 had impervious surface and 640 km of street length. TWPs were the main fraction (53 %) of
428 MPs in SDR sediments from street runoff, and their abundance can be related to the
429 characteristics of the contributing area such as high imperviousness and street density. Most of
430 the TWPs counted were within the lowest range examined (0.1 mm to 0.5 mm), and this can be
431 attributed to their easy transportation by surface runoff as a result of the frequent rainfall events.
432 TWPs at levels of 2,160 units/(kg·km²) of impervious area and 87.8 units/(kg·km) of street, and
433 TWP emissions ranging from 43.3 to 205.5 kg/day, demonstrate the significance of this kind of
434 pollution in urban areas and are, for the first time, measured as loading by unit of area or street
435 length. The annual flux was 7.8x10¹¹ units/(km²·year) for MPs among which 4.1x10¹¹
436 units/(km²·year) were for TWPs only. It is expected that MP and TWP pollution similar to what
437 has been found in the Jardim Arize SDR will be present in other urban areas with similar land-
438 use, around the world. Furthermore, we propose that further investigations consider the
439 imperviousness, street length and vehicle traffic as important features for runoff transport of
440 TWPs in urban areas and recommend SDRs as a strategy to collect and reduce MP pollution in
441 the environment.

442

443 **Acknowledgments**

444

445 Rodrigo B. Moruzzi is grateful to the São Paulo Research Foundation (Fundação de
446 Amparo à Pesquisa do Estado de São Paulo—FAPESP) Grant 2017/19195-7 for financial
447 support and to the Brazilian Federal Agency for Support and Evaluation of Graduate Education
448 (CAPES), in the scope of the Program CAPES-PrInt, process number 88887.571068/2020-00,
449 as well as to CNPq Grant numbers 309788/2021-8. Three anonymous reviewers are thanked

450 for their detailed and insightful review comments, which helped to improve the manuscript. Dr
451 L. Mbundi is acknowledged for language revision.

452

453 **References**

454

455 AMLURB, Autoridade Municipal de Limpeza Urbana, 2021. Coleta Resíduos Sólidos
456 Urbanos. <http://dados.prefeitura.sp.gov.br/dataset/coleta-de-residuos-solidos-urbanos>
457 (accessed 18 February 2022).

458 Anbumani, S., Kakkar, P., 2018. Ecotoxicological effects of microplastics on biota: a
459 review. *Environ. Sci. Pollut. Res.* 25, 14373-14396. [https://doi.org/10.1007/s11356-018-](https://doi.org/10.1007/s11356-018-1999-x)
460 [1999-x](https://doi.org/10.1007/s11356-018-1999-x)

461 Ballent, A., Corcoran, P.L., Madden, O., Helm, P.A., Longstaffe, F.J., 2016. Sources and sinks
462 of microplastics in Canadian Lake Ontario nearshore, tributary and beach sediments. *Mar.*
463 *Pollut. Bull.* 110, 383-395. <https://doi.org/10.1016/j.marpolbul.2016.06.037>

464 Browne, M.A., Crump, C.P., Niven, S.J., Teuten, E., Tonkin, A., Galloway, T., Thompson, R.,
465 2011. Accumulation of Microplastic on Shorelines Worldwide: Sources and Sinks. *Environ.*
466 *Sci. Technol.* 45, 9175-9179. <https://doi.org/10.1021/es201811s>

467 Canholi, A., 2014. Drenagem Urbana e Controle de Enchentes, 2^o ed. Oficina de Textos, São
468 Paulo.

469 CET, Companhia de Engenharia de Tráfego, 2019. Pesquisa de Mobilidade do Sistema Viário
470 Principal. <http://www.cetsp.com.br/sobre-a-cet/relatorios-corporativos.aspx> (accessed 16
471 March 2022).

472 Collaço, F.M.A., Simoes, S.G., Dias, L.P., Duic, N., Seixas, J., Bermann, C., 2019. The dawn
473 of urban energy planning—Synergies between energy and urban planning for São Paulo

- 474 (Brazil) megacity. *J. Clean. Prod.* 215, 458-479.
475 <https://doi.org/10.1016/j.jclepro.2019.01.013>
- 476 Couto Júnior, A.A., Conceição, F.T., Fernandes, A.M., Spatti Júnior, E.P., Lupinacci, C.M.,
477 Moruzzi, R.N. Land use changes associated with the expansion of sugar cane crops and
478 their influences on soil removal in a tropical watershed in São Paulo State (Brazil). *Catena*,
479 172, 313-323. <https://doi.org/10.1016/j.catena.2018.09.001>
- 480 Júnior, F.M., Magni, N.L.G., Piteri, R.F., Toledo, C.R.C., 2018. Governo do estado de São
481 Paulo. Secretaria de recursos hídricos, saneamento e obras. Departamento de águas e
482 energia elétrica. Centro tecnológico de hidráulica e recursos hídricos.
483 <https://drive.google.com/file/d/1JHG08Ql21xZM3jBoGZwgzVR4x2224eR2/view?usp=s>
484 [haring](#) (accessed 01 February 2021).
- 485 de Carvahó, A. R., Riem-Galliano, L., Ter Halle, A., & Cucherousset, J., 2022. Interactive effect
486 of urbanization and flood in modulating microplastic pollution in rivers. *Environ. Pollut.*
487 309, 119760. <https://doi.org/10.1016/j.envpol.2022.119760>
- 488 Di, M., Wang, J., 2018. Microplastics in surface waters and sediments of the Three Gorges
489 Reservoir, China. *Sci. Total Environ.* 616, 1620-1627.
490 <https://doi.org/10.1016/j.scitotenv.2017.10.150>.
- 491 Dikareva, N., Simon, K.S., 2019. Microplastic pollution in streams spanning an urbanisation
492 gradient. *Environ. Pollut.* 250, 292-299. <https://doi.org/10.1016/j.envpol.2019.03.105>
- 493 Dris, R., Gasperi, J., Tassin, B., 2018. Sources and fate of microplastics in urban areas: a focus
494 on Paris megacity. *Freshw. Microplastics.* 58, 69-83. [https://doi.org/10.1007/978-3-319-
495 61615-5_4](https://doi.org/10.1007/978-3-319-61615-5_4)
- 496 Fischer, E.K., Paglialonga, L., Czech, E., Tamminga, M., 2016. Microplastic pollution in lakes
497 and lake shoreline sediments—a case study on Lake Bolsena and Lake Chiusi (central
498 Italy). *Environ. Pollut.* 213, 648-657. <http://dx.doi.org/10.1016/j.envpol.2016.03.012>

- 499 Frias, J.P.G.L., Nash, R., 2019. Microplastics: finding a consensus on the definition. Mar.
500 Pollut. Bull. 138, 145-147. <https://doi.org/10.1016/j.marpolbul.2018.11.022>
- 501 Grbić, J., Helm, P., Athey, S., Rochman, C.M., 2016. Microplastics entering northwestern Lake
502 Ontario are diverse and linked to urban sources. Water Res. 174, 115623.
503 <https://doi.org/10.1016/j.watres.2020.115623>
- 504 Halle, L. L., Palmqvist, A., Kampmann, K., Jensen, A., Hansen, T., & Khan, F. R., 2021. Tire
505 wear particle and leachate exposures from a pristine and road-worn tire to *Hyalella azteca*:
506 comparison of chemical content and biological effects. Aquat. Toxicol. 232, 105769.
507 <https://doi.org/10.1016/j.aquatox.2021.105769>
- 508 Hong, Y., Bonhomme, C., Le, M., Chebbo, G., 2016. New insights into the urban washoff
509 process with detailed physical modelling. Sci. Total Environ. 573, 924-936.
510 <http://dx.doi.org/10.1016/j.scitotenv.2016.08.193>
- 511 Horton, A.A., Svendsen, C., Williams, R.J., Spurgeon, D.J., Lahive, E., 2017. Large
512 microplastic particles in sediments of tributaries of the River Thames, UK—Abundance,
513 sources and methods for effective quantification. Mar. Pollut. Bull. 114, 218-226.
514 <http://dx.doi.org/10.1016/j.marpolbul.2016.09.004>
- 515 Huang, H., Cheng, S., Wen, J., Lee, J., 2008. Effect of growing watershed imperviousness on
516 hydrograph parameters and peak discharge. Hydrol. Process. 22, 2075-2085.
517 <https://doi.org/10.1002/hyp.6807>
- 518 Jacobson, C.R., 2011. Identification and quantification of the hydrological impacts of
519 imperviousness in urban catchments: A review. J. Environ. Manag. 92, 1438-1448.
520 <https://doi.org/10.1016/j.jenvman.2011.01.018>
- 521 Järllskog, I., Strömvall, A., Magnusson, K., Galfi, H., Björklund, K., Polukarova, M., Garção,
522 R., Markiewicz, A., Aronsson M., Gustafsson, M., Norin, M., Blomc, L., Andersson-Sköld,
523 Y., 2021. Traffic-related microplastic particles, metals, and organic pollutants in an urban

- 524 area under reconstruction. *Sci. Total Environ.* 774, 145503.
525 <https://doi.org/10.1016/j.scitotenv.2021.145503>
- 526 Järllskog, I., Strömvall, A., Magnusson, K., Gustafsson, M., Polukarova, M., Galfi, H.,
527 Aronsson M., Andersson-Sköld, Y., 2020. Occurrence of tire and bitumen wear
528 microplastics on urban streets and in sweepsand and washwater. *Sci. Total Environ.* 729,
529 138950. <https://doi.org/10.1016/j.scitotenv.2020.138950>
- 530 Jiang, C., Yin, L., Li, Z., Wen, X., Luo, X., Hu, S., Yang, H., Long, Y., Deng, B., Huang, L.,
531 Liu, Y., 2019. Microplastic pollution in the rivers of the Tibet Plateau. *Environ. Pollut.*
532 249, 91-98. <https://doi.org/10.1016/j.envpol.2019.03.022>
- 533 Kawakubo, F., Morato, R., Martins, M., Mataveli, G., Nepomuceno, P., Martines, M., 2019.
534 Quantification and Analysis of Impervious Surface Area in the Metropolitan Region of São
535 Paulo, Brazil. *Remote Sens.* 11, 944. <https://doi.org/10.3390/rs11080944>
- 536 Klein, S., Worch, E., Knepper, T.P., 2015. Occurrence and spatial distribution of microplastics
537 in river shore sediments of the Rhine-Main area in Germany. *Environ. Sci. Technol.* 49,
538 6070-6076. <https://doi.org/10.1021/acs.est.5b00492>
- 539 Klöckner, P., Seiwert, B., Eisentraut, P., Braun, U., Reemtsma, S.W., 2020. Characterization
540 of tire and road wear particles from road runoff indicates highly dynamic particle
541 properties. *Water Res.* 185, 116262. <https://doi.org/10.1016/j.watres.2020.116262>
- 542 Knight, L.J., Parker-Jurd, F.N.F., Al-Sid-Cheikh, M., Thompson, R.C., 2020. Tyre wear
543 particles: an abundant yet widely unreported microplastic? *Environ. Sci. Pollut. Res.* 27,
544 18345-18354. <https://doi.org/10.1007/s11356-020-08187-4>
- 545 Kole, P.J., Löhr, A.J, Van Belleghen, F.G.A.J., Ragas, A.M.J., 2017. Wear and tear of tyres: a
546 stealthy source of microplastics in the environment. *Int. J. Environ. Res. Publ. Health.* 14,
547 1265, 2017. <https://doi.org/10.3390/ijerph14101265>

- 548 Koutnik, V.S., Leonard, J., Alkidim, S., DePrima, F.J., Ravi, S., Hoek, E.M.V., Mohanty, S.K.,
549 2021. Distribution of microplastics in soil and freshwater environments: Global analysis
550 and framework for transport modeling. *Environ. Pollut.* 274, 116552.
551 <https://doi.org/10.1016/j.envpol.2021.116552>
- 552 Koutnik, V.S., Leonard, J., Glasman, J.B., Brar, J., Koydemir, H.C., Novosselov, A., Bertel,
553 R., Tseng, D., Ozcan, A., Ravi, S., Mohanty, S.K., 2022. Microplastics retained in
554 stormwater control measures: Where do they come from and where do they go? *Water Res.*
555 210, 118008. <https://doi.org/10.1016/j.watres.2021.118008>
- 556 Kumar, M., Chen, H., Sarsaiya, S., Qin, S., Liu, H., Awasthi, M.K., Kumar, S., Singh, L.,
557 Zhang, Z., Bolan, N.S., Pandey, A., Varjani, S., Taherzadeh, M.J., 2021. Current research
558 trends on micro-and nano-plastics as an emerging threat to global environment: A
559 review. *J. Hazard. Mater.* 409, 124967. <https://doi.org/10.1016/j.jhazmat.2020.124967>
- 560 Lange, K., Magnusson, K., Viklander, M., Blecken, G.T., 2021. Removal of rubber, bitumen
561 and other microplastic particles from stormwater by a gross pollutant trap-bioretention
562 treatment train. *Water Res.* 202, 117457. <https://doi.org/10.1016/j.watres.2021.117457>
- 563 Leads, R.R., Weinstein, J.E., 2019. Occurrence of tire wear particles and other microplastics
564 within the tributaries of the Charleston Harbor Estuary, South Carolina, USA. *Mar. Pollut.*
565 *Bull.* 145, 569-582. <https://doi.org/10.1016/j.marpolbul.2019.06.061>
- 566 Li, J., Huang, W., Xu, Y., Jin, A., Zhang, D., Zhang, C., 2020. Microplastics in sediment cores
567 as indicators of temporal trends in microplastic pollution in Andong salt marsh, Hangzhou
568 Bay, China. *Reg. Stud. Mar. Sci.* 35, 101149. <https://doi.org/10.1016/j.rsma.2020.101149>
- 569 Li, Y., Shi, T., Li, X., Sun, H., Xia, X., Ji, X., Zhang, J., Liu, M., Lin, Y., Zhang, R., Zheng,
570 Y., Tang, J., 2022. Inhaled tire-wear microplastic particles induced pulmonary fibrotic
571 injury via epithelial cytoskeleton rearrangement. *Environ. Int.* 164, 107257.
572 <https://doi.org/10.1016/j.envint.2022.107257>

- 573 Lima, G.N., Rueda, V.O.M., 2018. The urban growth of the metropolitan area of Sao Paulo and
574 its impact on the climate. *Weather Clim. Extrem.* 21, 17-26.
575 <https://doi.org/10.1016/j.wace.2018.05.002>
- 576 Lima, G.N., Lombardo, M.A., Magaña, V., 2018. Urban water supply and the changes in the
577 precipitation patterns in the metropolitan area of São Paulo–Brazil. *Appl. Geogr.* 94, 223-
578 229. <https://doi.org/10.1016/j.apgeog.2018.03.010>
- 579 Lin, L., Pan, X., Zhang, S., Li, D., Zhai, W., Wang, Z., Tao, J., Mi, C., Li, Q., Crittenden, J.C.,
580 2021. Distribution and source of microplastics in China's second largest reservoir-
581 Danjiangkou Reservoir. *J. Environ. Sci.* 102, 74-84.
582 <https://doi.org/10.1016/j.jes.2020.09.018>
- 583 Liu, S., Jian, M., Zhou, L., Li, W., 2019a. Distribution and characteristics of microplastics in
584 the sediments of Poyang Lake, China. *Water Sci. Technol.* 79, 1868-1877.
585 <https://doi.org/10.2166/wst.2019.185>
- 586 Liu, F., Vianello, A., Vollersten, J., 2019. Retention of microplastics in sediments of urban and
587 highway stormwater retention ponds. *Environ. Pollut.* 255, 113335.
588 <https://doi.org/10.1016/j.envpol.2019.113335>
- 589 Lupinacci, C., Conceição, F.T., Paschoal, L.G., 2022. Geomorphic responses due to the second-
590 largest global producer of ceramic tiles in the State of São Paulo, Brazil. *Catena* 218,
591 106560. <https://doi.org/10.1016/j.catena.2022.106550>
- 592 Lupinacci, C., Conceição, F.T., Simon, A.L.H., Filho, A.P., 2017. Land use changes due to
593 energy policy as a determining factor for morphological processes in fluvial systems in São
594 Paulo State, Brazil. *Earth Surf. Process. Landf.* 42, 2402-2413.
595 <https://doi.org/10.1002/esp.4200>

- 596 Ma, B., Xue, W., Hu, C., Liu, H., Qu, J., Li, L., 2019. Characteristics of microplastic removal
597 via coagulation and ultrafiltration during drinking water treatment. *Chem. Eng. J.* 359, 159-
598 167. <https://doi.org/10.1016/j.cej.2018.11.155>
- 599 Martins, M.H., Morato, R.G., Kawakubo, F.S., 2018. Mapping Impervious Surface Areas Using
600 Orthophotos, Satellite Imagery and Linear Regression. *Rev. Dep. Geogr.* 35, 91-101.
601 <https://doi.org/10.11606/rdg.v35i0.131542>
- 602 Miller, J.D., Kim, H., Kjeldsen, T.R., Packman, J., Grebby, S., Dearden, R., 2014. Assessing
603 the impact of urbanisation on storm runoff in a peri-urban catchment using historical
604 change in impervious cover. *J. Hydrol.* 515, 59-70.
605 <http://dx.doi.org/10.1016/j.jhydrol.2014.04.011>
- 606 Moruzzi, R.B., Speranza, L.G., Conceição, F.T., Martins, S.T.S., Busquets, R., Campos, L.C.,
607 2020. Stormwater detention reservoirs: an opportunity for monitoring and a potential site
608 to prevent the spread of urban microplastics. *Water.* 12, 1994.
609 <https://doi.org/10.3390/w12071994>
- 610 Nel, H.A., Dalu, T., Wasserman, R.J., 2018. Sinks and sources: Assessing microplastic
611 abundance in river sediment and deposit feeders in an Austral temperate urban river
612 system. *Sci. Total Environ.* 612, 950-956.
613 <http://dx.doi.org/10.1016/j.scitotenv.2017.08.298>
- 614 Nematollahi, M.J., Keshavarzi, B., Mohit, F., Moore, F., Busquets, R., 2022. Microplastic
615 occurrence in urban and industrial soils of Ahvaz metropolis: a city with a sustained record
616 of air pollution. *Sci. Total Environ.* 819, 152051.
617 <http://dx.doi.org/10.1016/j.scitotenv.2021.152051>
- 618 Niu, J., Gao, B., Wu, W., Peng, W., Xu, D., 2022. Occurrence, stability and source identification
619 of small size microplastics in the Jiayan reservoir, China. *Sci. Total Environ.* 807, 150832.
620 <https://doi.org/10.1016/j.scitotenv.2021.150832>

- 621 Peponis, J., Allen, D., French, S. Scoppa, M., Brown, J., 2007. Street connectivity and urban
622 density: spatial measures and their correlation. In: A.S. Kubat, O. Ertekin, Y.I. Guney and
623 E. Eyuboglu (SEMSEM) Proceedings of the 6th International Space Syntax Symposium,
624 1–12.
625 <http://citeseerx.ist.psu.edu/viewdoc/download?doi=10.1.1.550.761&rep=rep1&type=pdf>
626 (accessed 18 February 2022).
- 627 Ramezani, M.R., Yu, B., Che, Y., 2021. Prediction of Total Imperviousness from Population
628 Density and Land Use Data for Urban Areas (Case Study: South East Queensland,
629 Australia). Appl. Sci. 11, 10044. <https://doi.org/10.3390/app112110044>
- 630 Rodrigues, M.O., Abrantes, N., Gonçalves, F.J.M, Nogueira, H., Marques, J.C., Gonçalves,
631 A.M.M., 2018. Spatial and temporal distribution of microplastics in water and sediments
632 of a freshwater system (Antuã River, Portugal). Sci. Total Environ. 633, 1549-1559.
633 <https://doi.org/10.1016/j.scitotenv.2018.03.233>
- 634 Santos, P.B., Maziviero, M.C., 2016. Impacts of inclusion of local big pools scale: the Retention
635 Reservoir case RC5 – Taboão. Arquit. Urban. 17, 22-44.
636 São Paulo, 2107. Informes Urbanos: A dinâmica do IDH-M e suas dimensões entre 2000 e 2010
637 no município de São Paulo.
638 https://www.prefeitura.sp.gov.br/cidade/secretarias/upload/Informes_Urbanos/29_Dimensoes_IDH-M.pdf (accessed 18 February 2022).
- 639
- 640 Simas, I.T.H., Rodrigues, C., 2020. Socio-spatial vulnerability mapping: integrated analysis
641 between social vulnerability and flooding susceptibility in an urbanized hydrographic basin
642 of São Paulo. Rev. Fr.-Bras. Geogr. 45, 29408. <https://doi.org/10.4000/confins.29408>
- 643 Simas, I.T.H, Rodrigues, C., Neto, J.L.A., 2017. Análise retrospectiva de inundação na bacia
644 do Rio Aricanduva, São Paulo. Bol. Paul. Geogr. 97, 1-20.

- 645 Skaf, D.W., Punzi, V.L., Rolle, J.T., Kleinberg, K.A., 2020. Removal of micron-sized
646 microplastic particles from simulated drinking water via alum coagulation. *Chem. Eng. J.*
647 386, 123807. <https://doi.org/10.1016/j.cej.2019.123807>
- 648 Smyth, K., Drake, J., Li, Y., Rochman, C., Seters, T.V., Passeport, E., 2021. Bioretention cells
649 remove microplastics from urban stormwater. *Water Res.* 191, 116785.
650 <https://doi.org/10.1016/j.watres.2020.116785>
- 651 Sobrinho P., Tsutiya M., 1999. *Coleta de Transporte de Esgoto Sanitário*, 1^o ed. Escola
652 Politécnica USP, São Paulo.
- 653 Sun, J., Ho, S.H., Niu, X., Xu, H., Qu, L., Shen, Z., Cao, J., Chuang, H., Ho, K., 2022.
654 Explorations of tire and road wear microplastics in road dust PM_{2.5} at eight megacities in
655 China. *Sci. Total Environ.* 823, 153717. <https://doi.org/10.1016/j.envint.2022.107257>
- 656 Triebkorn, R., Braunbeck, T., Grummt, T., Hanslik, L., Huppertsberg, S., Jekel, M., Knepper,
657 T.P., Kraus, S., Müller, Y.K., Pittroff, M., Ruhl, A.S., Schmiege, H., Schür, C., Strobel, C.,
658 Wagner, M., Zumbülte, N., Köhler, H.R., 2019. Relevance of nano- and microplastics for
659 freshwater ecosystems: a critical review. *TrAC Trends Anal. Chem.* 110, 375-392.
660 <https://doi.org/10.1016/j.trac.2018.11.023>
- 661 Vaughan, R., Turner, S.D., Rose, N.L., 2017. Microplastics in the sediments of a UK urban
662 lake. *Environ. Pollut.* 229, 10-18. <http://dx.doi.org/10.1016/j.envpol.2017.05.057>
- 663 Verschoor, A. J., 2015. Towards a definition of microplastics: Considerations for the
664 specification of physico-chemical properties. National Institute for Public Health and the
665 Environment. Ministry of Infrastructure and the Environment, The Netherlands.
666 <http://www.rivm.nl/>
- 667 Wang, J., Peng, J., Tan, Z., Gao, Y., Zhan, Z., Chen, Q., Cai, L., 2017. Microplastics in the
668 surface sediments from the Beijiang River littoral zone: composition, abundance, surface

- 669 textures and interaction with heavy metals. *Chemosphere*. 171, 248-258.
670 <http://dx.doi.org/10.1016/j.chemosphere.2016.12.074>
- 671 Werbowski, L.M., Gilbreath, A.N., Munno, K., Zhu, X., Gbric, J., Wu, T., Sutton, R., Sedlak,
672 M.D., Deshpande, A.D., Rochman, C.M., 2021. Urban Stormwater Runoff: A Major
673 Pathway for Anthropogenic Particles, Black Rubbery Fragments, and Other Types of
674 Microplastics to Urban Receiving Waters. *ACS EST Water*. 1, 1420-1428.
675 <https://doi.org/10.1021/acsestwater.1c00017>
- 676 Wik, A., Dave, G., 2009. Occurrence and effects of tire wear particles in the environment—A
677 critical review and an initial risk assessment. *Environ. Pollut.* 157, 1-11.
678 <https://doi.org/10.1016/j.envpol.2008.09.028>
- 679 Wu, W., Li, C., Liu, M., Hu, Y., Xiu, C., 2020. Change of impervious surface area and its
680 impacts on urban landscape: an example of Shenyang between 2010 and 2017. *Ecosyst.*
681 *Health Sustain.* 6, 1767511. <https://doi.org/10.1080/20964129.2020.1767511>
- 682 Yan, H., Zhang, L., Liu, L., Wen, S., 2021. Investigation of the external conditions and material
683 compositions affecting the formation mechanism and size distribution of tire wear
684 particles. *Atmos. Environ.* 244, 118018. <https://doi.org/10.1016/j.atmosenv.2020.118018>
- 685 Zhang, X., Chen, P., Liu, P., 2020. Review of Tires Wear Particles Emission Research
686 Status. *IOP Conf. Ser.: Earth Environ. Sci.* 555, 012062.
687 <https://iopscience.iop.org/article/10.1088/1755-1315/555/1/012062>
- 688 Zheng, Y., Li, J., Cao, W., Jiang, F., Zhao, C., Ding, H., Wang, M., Gao, F., Sun, C., 2020.
689 Vertical distribution of microplastics in bay sediment reflecting effects of sedimentation
690 dynamics and anthropogenic activities. *Mar. Pollut. Bull.* 152, 110885.
691 <https://doi.org/10.1016/j.marpolbul.2020.110885>
- 692 Ziajahromi, S., Drapper, D., Hornbuckle, A., Rintoul, L., Leusch, F.D.L., 2020. Microplastic
693 pollution in a stormwater floating treatment wetland: Detection of tyre particles in

694 sediment. Sci. Total Environ. 713, 136356.

695 <https://doi.org/10.1016/j.scitotenv.2019.136356>

696

697

698

699

700

701

702

703

704

705

706

707

708

709

710

711

712

713

714

715

716

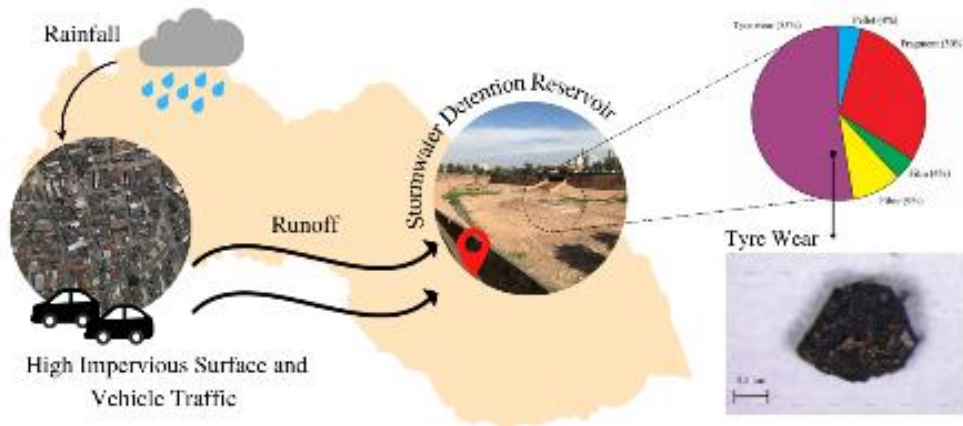
717

718

Graphical Abstract and Figures

719

720

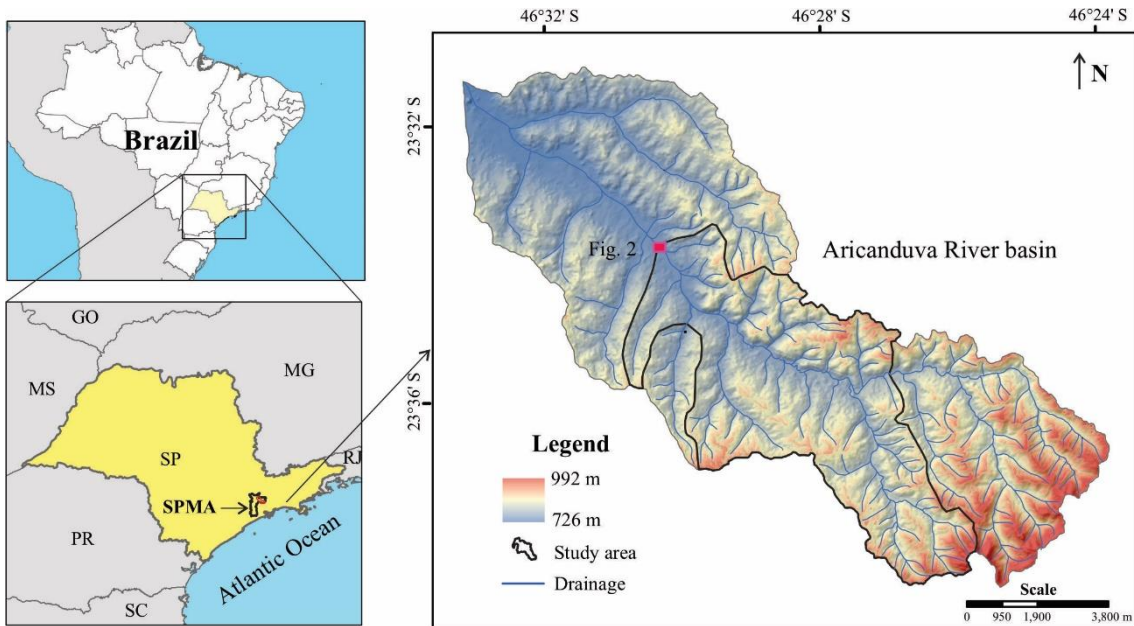


721

722

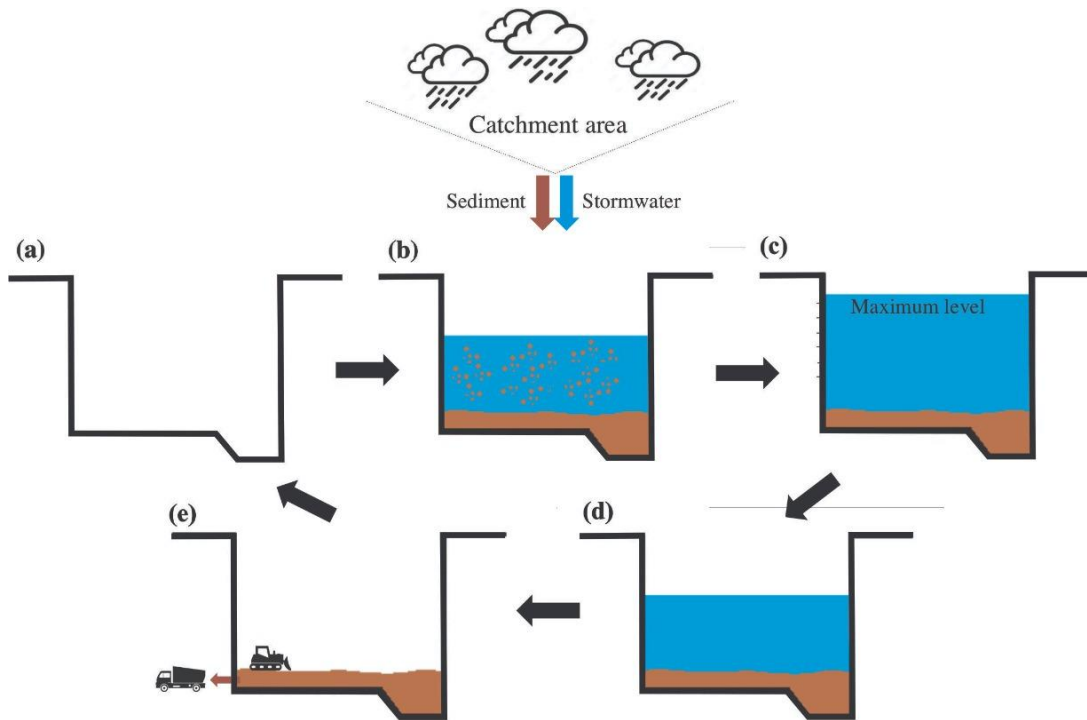
723

724



725

726 Figure 1 – Maps of the São Paulo Metropolitan Area (SPMA) (left) with digital elevation model
 727 (USGS/SRTM3”) using 30 m of resolution for Aricanduva River basin (right). The Aricanduva
 728 River basin contributes to runoff into SDR.



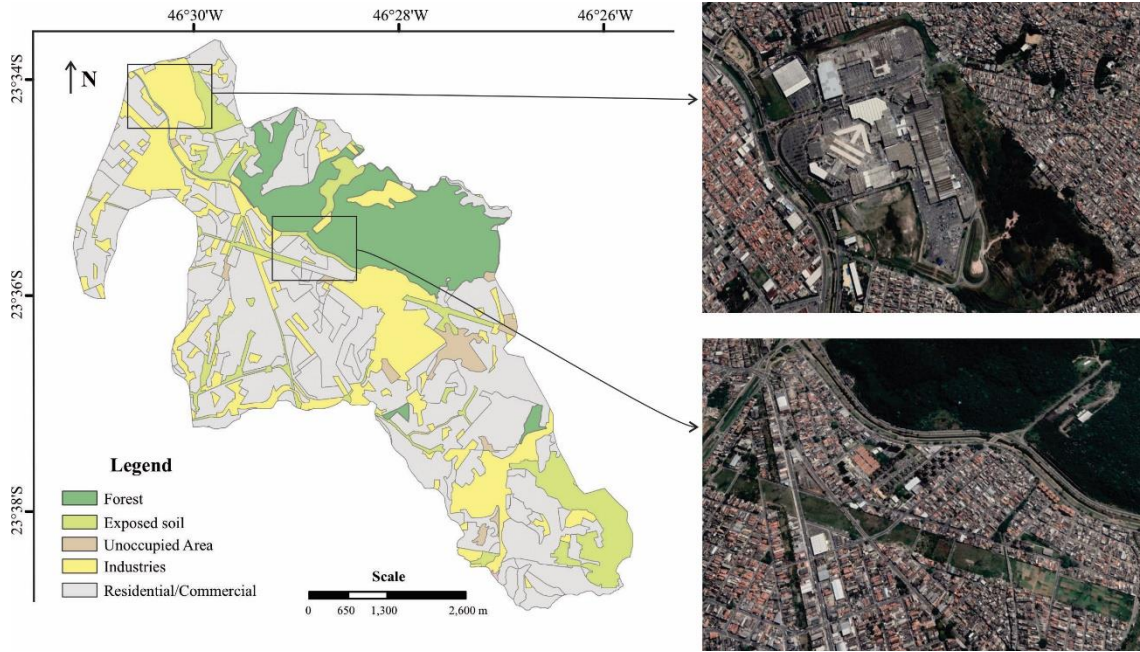
729

730 Figure 2 – Schematic sequential operation for the off-line Jardim Arize SDR. Empty SDR (a)
 731 receives runoff from side weir (b) up to the established maximum level (c) from where water is
 732 pumped out back to river (d), and remaining sediment is scratched and put aside, where the
 733 sediment is removed to a controlled landfill. The frequency of cycles depends upon the rainfall
 734 and the amount of sediment carried by runoff.



735

736 Figure 3 – Jardim Arize SDR marked with continuous red line, with the image from Google
 737 Earth Pro - 06/28/2020 (a). Overview of the Jardim Arize SDR, with the sediment scratched
 738 and put aside for removal (red circle) (b). Detail of the circled area (c).

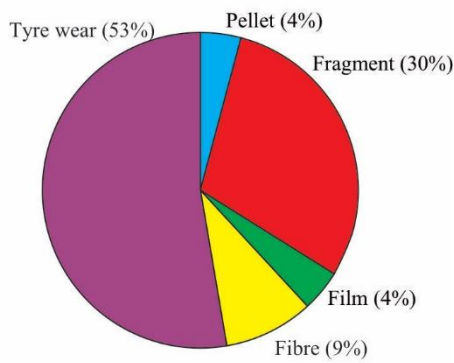


739

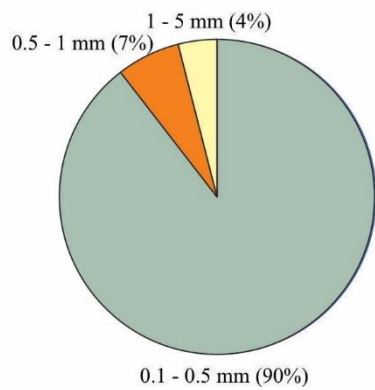
740 Figure 4 - Land use mapping of the catchment area, with details extracted from Google Earth

741 Pro - 28/06/2020.

(a)



(b)

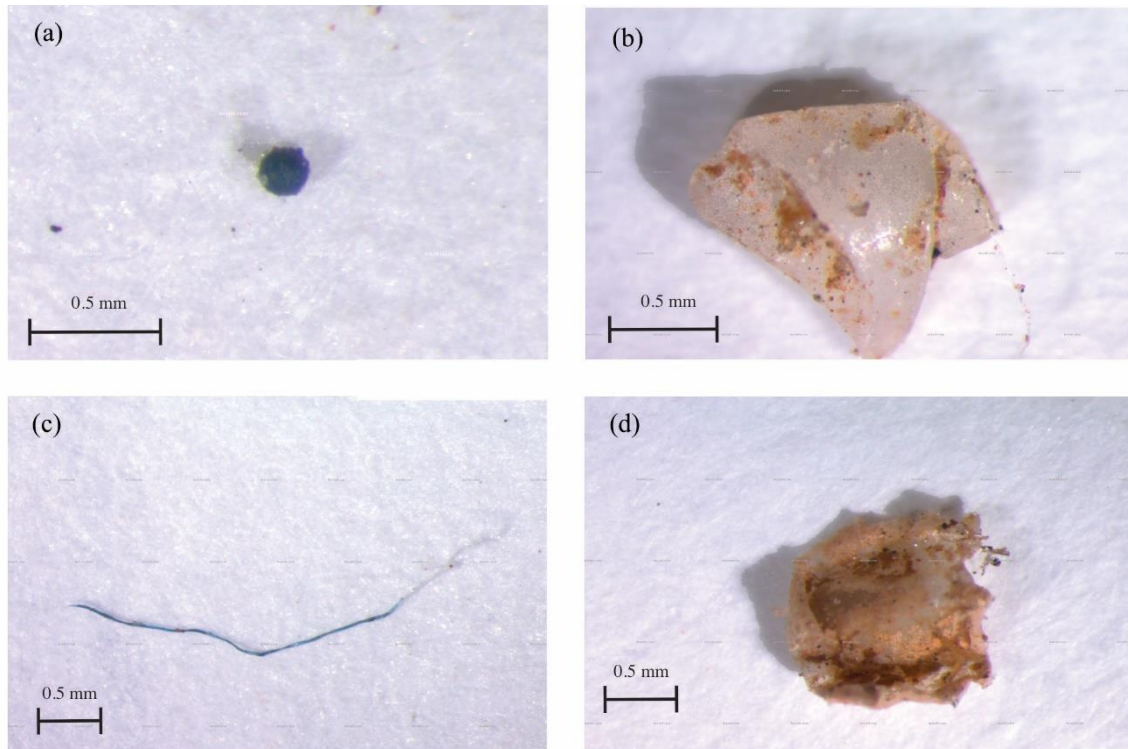


742

743 Figure 5 – Distribution of MPs, considering type (a) and size (b), in sediments collected in the Jardim

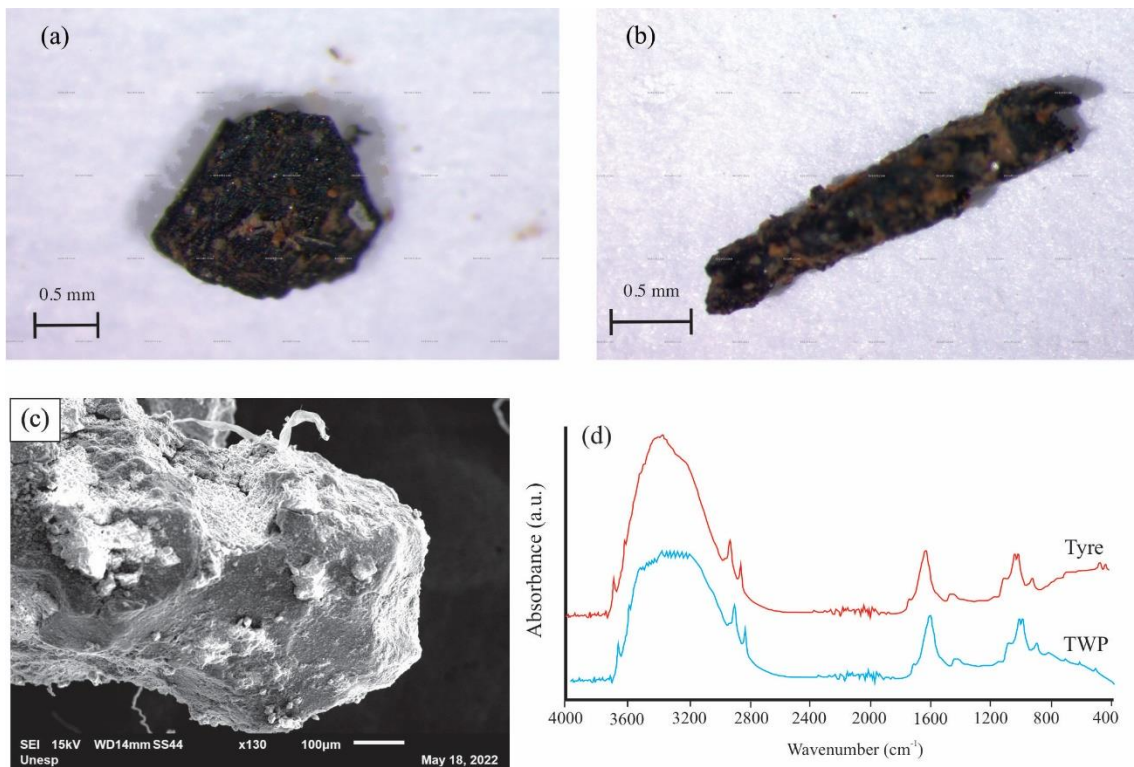
744 Arize SDR.

745



746

747 Figure 6 – Examples of different types and shape of MPs in sediments collected in the Jardim Arize
 748 SDR: pellet (a), fragments (b), fibre (c) and film (d).



749

750 Figure 7 – Examples of MPs identified as TWPs in the Jardim Arize SDR. Optical microscopy images
 751 (a and b) and SEM images showing the morphology of TWPs (c). ATR FTIR spectra comparing tyre
 752 standard with TWPs (d).

753 Table 1. Characteristics of MPs found in sediments collected in the Jardim Arize SDR
 754 classified by type and size (units/kg). The values in brackets correspond to relative standard
 755 variations from three sediment samples, where each sample was 2 kg taken from the surface of
 756 the bottom of the SDR.

757

Type\Size	0.1–0.5 mm	0.5–1 mm	1.0–5.0 mm	Total (units/kg)
Tyre wear	55,294 ($\pm 46\%$)	1800 ($\pm 33\%$)	367 ($\pm 71\%$)	57,461 ($\pm 45\%$)
Fragment	30,089 ($\pm 41\%$)	1550 ($\pm 39\%$)	817 ($\pm 90\%$)	32,456 ($\pm 41\%$)
Fibre	5122 ($\pm 71\%$)	2506 ($\pm 55\%$)	2394 ($\pm 60\%$)	10,022 ($\pm 47\%$)
Film	2622 ($\pm 47\%$)	1250 ($\pm 78\%$)	750 ($\pm 64\%$)	4622 ($\pm 52\%$)
Pellet	4528 ($\pm 38\%$)	–	–	4528 ($\pm 38\%$)
Total	97,656 ($\pm 38\%$)	7106 ($\pm 33\%$)	4328 ($\pm 65\%$)	109,089 ($\pm 38\%$)

758

759 Table 2. MPs (units/kg) in sediments sampled in urban areas found in previous investigations
 760 and this study.

Location	Country	MPS (units/kg)	Reference
Jiaozhou Bay	China	≤ 27	Zheng et al. (2020)
Streams in Auckland	New Zealand	≤ 80	Dikareva and Simon (2019)
Bloukrans River	South Africa	≤ 160	Nel, Dalu and Wasserman (2018)
Tibet Plateau	China	≤ 195	Jiang et al. (2019)
Lake Bolsena and Chiusi	Italy	≤ 266	Fischer et al. (2016)
Three Gorges Reservoir	China	≤ 300	Di and Wang (2018)
Edgbaston Pool	UK	≤ 300	Vaughan et al. (2017)
Beijiang River	China	≤ 544	Wang et al. (2017)
Antuã River	Portugal	≤ 1265	Rodrigues et al. (2018)
SCMs in Los Angeles	EUA	≤ 2784	Koutnik et al. (2022)
Lake Poyang	China	≤ 3153	Liu et al. (2019a)
Danjiangkou Reservoir	China	≤ 3237	Lin et al. (2021)
Rhine e Main River	Germany	≤ 3763	Klein et al. (2015)
Jiayan Reservoir	China	$\leq 15,700$	Niu et al. (2022)
Lake Ontario	Canada	$\leq 28,000$	Ballent et al. (2016)
Poá SDR	Brazil	$\leq 57,542$	Moruzzi et al. (2020)
Stormwater Pound	Denmark	$\leq 127,986$	Liu et al. (2019)
Jardim Arize SDR	Brazil	$\leq 109,089$	Present study

761

Supplementary Material

762

763

764

765

766

Table S.1 – Surface area by land use classes in the study area.

767

Land use	Area (km²)	Area (%)
Water bodies	0.06	0.15
Reforest	5.58	15.32
Exposed soil	3.47	9.52
Unoccupied area	0.71	1.94
Residential/commercial	19.18	52.67
Industrial	7.42	20.37
Total	36.43	100.00

768

769

770

771 Table S.2 - Rainfall intensity (mm/hour) for a return period (TR) between 2 and 10 years and
772 duration of 10, 20, 30 and 60 min for São Paulo.

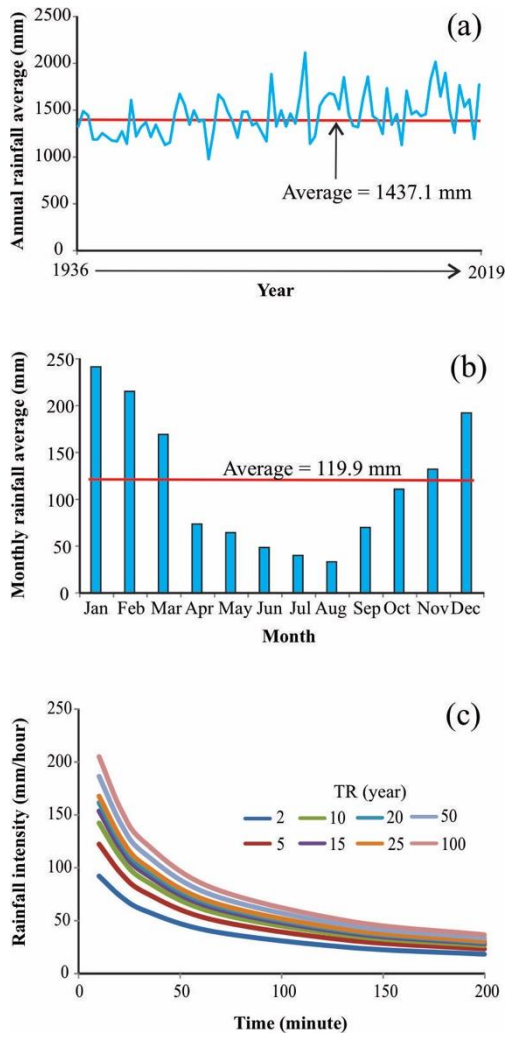
773

Duration (min)	TR (years)			
	2	5	6	10
10	94.3	124.3	129.6	144.1
20	73.1	97.4	101.8	113.5
30	60.0	80.5	84.2	94.1
60	39.6	53.7	56.2	63.0

774

775

776



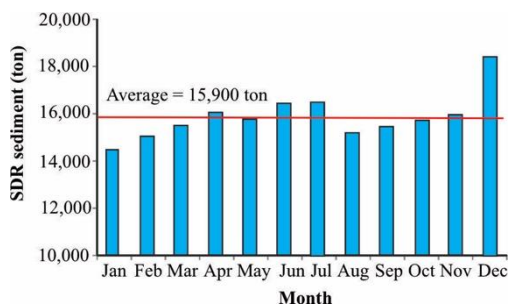
777

778

779 Figure S.1 – Annual (a) and monthly (b) rainfall average in the period between 1936 and 2019
 780 (DAEE, 2020). Rainfall intensity with different return period (TR) (c).

781

782



783

784

785 Figure S.2 – Monthly average of sediments removed from SDRs in São Paulo, between 2013
 786 and 2020 (AMLURB, 2022).

787